Kinetic Mechanism of *Escherichia coli* Glutamine Synthetase†

Thomas D. Meek and Joseph J. Villafranca*,‡

ABSTRACT: The kinetic mechanism of *Escherichia coli* glutamine synthetase (unadenylylated) has been determined at pH 7.5, 25 °C. For both the forward and reverse biosynthetic reactions, initial velocity, product (forward reaction only), and dead-end inhibition patterns are consistent with preferred ordered addition of MgATP, glutamate, and ammonia, followed by the preferred ordered release of P_i, glutamine, and MgADP. These data and the previously published equilibrium isotope exchange data, when taken together, provide an overall mechanism that is steady-state random with strongly preferred ordered substrate addition and product release. Initial velocity data of $1/v$ vs. $1/[NH_4^+]$ are nonlinear (concave downward) when glutamate is subsaturating but linear at saturating glutamate levels. These experiments suggest negatively cooperative binding of NH_4^+. This kinetic mechanism is in accord with the initial formation of the proposed γ-glutamyl phosphate intermediate from MgATP and glutamate, followed by ammonia attack to produce glutamine and P_i. Two new competitive inhibitors of *E. coli* glutamine synthetase, 3-amino-3-carboxypropanesulfonamide and 2-amino-4-phosphonobutyric acid, have been characterized. The low inhibition constants ($K_i \simeq 50$ μM) of these glutamate analogues suggest that they may be structural mimics of a tetrahedral transition state in the catalytic mechanism.

Glutamine synthetase from *Escherichia coli* is composed of 12 equivalent subunits and has a molecular weight of 600 000. It exists in both unmodified and covalently modified forms with the modification being enzymatic adenylylation of a single tyrosyl residue per subunit (Stadtman & Ginsburg, 1974). Of the several reactions that it catalyzes, the physiologically important one is the biosynthesis of glutamine from glutamate which requires two divalent cations per subunit (eq 1). Although several chemical mechanisms have been pro-

$$\text{MgATP} + \text{L-Glu} + NH_4^+ \rightarrow \text{MgADP} + \text{L-Gln} + P_i \quad (1)$$

posed for the biosynthetic reaction, there is strong evidence for the initial formation of a γ-glutamyl phosphate intermediate from MgATP and glutamate (eq 2), followed by phos-

$$\text{MgATP} + \text{Glu} \rightarrow \text{MgADP}\cdot\gamma\text{-Glu-P} \quad (2)$$

phate displacement by ammonia to give inorganic phosphate and glutamine (eq 3) (Midlefort & Rose, 1976; Krishnaswamy

$$\text{MgADP}\cdot\gamma\text{-Glu-P} + NH_3 \rightarrow \text{MgADP} + \text{Gln} + P_i \quad (3)$$

et al., 1962; Weisbrod & Meister, 1973; Tsuda et al., 1971). No ATP ⇄ ADP isotope exchange is observed in the absence of ammonia, as might be expected for the first partial reaction (eq 2) (Wedler & Boyer, 1972), but it is very likely that this exchange does not occur because the putative E·MgADP·γ-Glu-P complex cannot release MgADP prior to its reaction with ammonia.

To the kineticist, the first level of understanding the actual chemical mechanism of an enzymatic reaction is knowledge of the kinetic mechanism, i.e., the order of substrate addition and product release on the enzyme surface as determined by steady-state methods. With this information at hand, one can minimize the number of possible chemical mechanisms and suggest likely reaction intermediates as indicated by the sequence of substrate interactions on the enzyme. Previous kinetic studies with glutamine synthetase from bacterial and mammalian sources indicate a random ter-ter mechanism in which the catalytic steps are not solely rate limiting (Wedler & Boyer, 1972; Allison et al., 1977; Timmons et al., 1974). For the *E. coli* enzyme, this mechanism is based on equilibrium isotope exchange data (Wedler & Boyer, 1972) and fluorometric studies (Timmons et al., 1974). However, the steady-state random mechanism has not yet been demonstrated for the bacterial enzyme by classical steady-state techniques such as initial velocity and product inhibition experiments.

In this report, we present a steady-state analysis of unadenylylated *E. coli* glutamine synthetase, employing initial velocity and inhibition methods for both the forward and reverse biosynthetic reactions. The kinetic mechanism that is most consistent with our data is steady-state ordered, thus differing with those mechanisms proposed in the cited literature. However, all the data can be accommodated by a steady-state random mechanism with a preferred ordered pathway, and the arguments germane to this mechanism are discussed in this paper. Also, in the course of this study we have used two newly characterized competitive inhibitors of *E. coli* glutamine synthetase, DL-3-amino-3-carboxypropanesulfonamide (ACPS,[1] I; Meek & Villafranca, 1978) and DL-

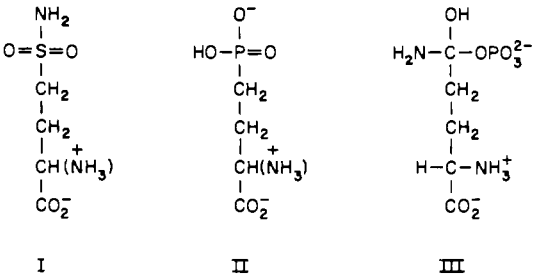

I II III

2-amino-4-phosphonobutyric acid (APBA, II). These glutamate analogues act as dead-end inhibitors (Fromm, 1967), and greatly assist in the assignment of the kinetic mechanism. Since both ACPS and APBA have tetrahedral geometry at their δ atoms, the tight binding of these inhibitors, as indicated by their inhibition constants, suggests that ammonia attack on γ-glutamyl phosphate results in the formation of a reactive

† From the Department of Chemistry, The Pennsylvania State University, University Park, Pennsylvania 16802. *Received April 15, 1980.* Supported in part by the U.S. Public Health Service (GM23529) and the National Science Foundation (PCM-7807845). A preliminary report of these data has been previously presented (Meek, 1980).

‡ J.J.V. is an Established Investigator of the American Heart Association.

[1] Abbreviations used: ACPS, DL-3-amino-3-carboxypropanesulfonamide; APBA, DL-2-amino-4-phosphonobutyric acid; PEP, phosphoenolpyruvate; Hepes, *N*-(2-hydroxyethyl)piperazine-*N*′-2-ethanesulfonic acid.

0006-2960/80/0419-5513$01.00/0

intermediate with tetrahedral geometry at its δ-carbon atom (III).

Experimental Procedures

Materials and Methods. Glutamine synthetase was isolated from *Escherichia coli* in a state of low adenylylation (average value of either 1.7 or 3.3 adenyl groups per 12 subunits) by either of two previously described methods (Shapiro & Stadtman, 1970; Miller et al., 1974). The enzyme activity (γ-glutamyl transferase assay) and state of adenylylation (spectrophotometric assay) were determined by the procedures of Shapiro & Stadtman (1970). Protein concentrations were measured by the method of Lowry et al. (1951) and by spectral measurements as described by Ginsburg et al. (1970). DL-3-Amino-3-carboxypropanesulfonamide was synthesized according to the procedures of Reisner (1956) and Mosher et al. (1958), mp 233–235 °C dec (reported 232 °C dec), and the purity of the compound was confirmed by IR and microanalysis. (Anal. Calcd for $C_4H_{10}N_2O_4S$: C, 26.37; H, 5.53; N, 15.38; S, 17.60. Found: C, 26.08; H, 5.34; N, 15.21; S, 17.61.) DL-2-Amino-4-phosphonobutyric acid was purchased from Calbiochem. Imidazole and 2-methylimidazole were purchased from Aldrich. All other chemicals were Sigma products.

Enzyme Assays. Initial velocities with glutamine synthetase were measured spectrophotometrically by using the pyruvate kinase–lactate dehydrogenase coupling system for the forward reaction and the hexokinase–glucose-6-phosphate dehydrogenase coupling system for the reverse reaction. A Beckman DU monochrometer equipped with a Gilford 2000 optical density converter and a 10-mV recorder was used to follow the reaction at 340 nm. The reaction temperature for all experiments was maintained at 25 ± 1 °C by a constant temperature water circulator.

In a typical forward reaction assay, each 1.0-mL cuvette contained 33 mM imidazole, 33 mM 2-methylimidazole, 33 mM 2,4-dimethylimidazole (pH 7.5), 0.1 M KCl, 33 μg each of pyruvate kinase and lactate dehydrogenase, 1 mM PEP, 0.19 mM NADH, 25 mM $MgCl_2$, and various concentrations of the substrates and inhibitors. The reactions were initiated by the addition of 2 μg of glutamine synthetase.

In the presence of added MgADP, initial rates were measured by the colorimetric determination of phosphate (Woolfolk et al., 1966). Each 0.2-mL assay mixture contained 0.1 M mixed imidazoles (pH 7.5), 0.1 M KCl, 10 mM excess $MgCl_2$, and various concentrations of the substrates and ADP. At 25 °C, the reaction was initiated with 1–5 μg of glutamine synthetase and quenched after equal time intervals with 1.8 mL of 0.8% $FeSO_4 \cdot 3H_2O$ in 0.015 N H_2SO_4. Color was developed with 0.15 mL of 6.6% $(NH_4)_6Mo_7O_{24} \cdot 4H_2O$ in 7.5 N H_2SO_4 and read at 660 nm.

For reverse reaction assays, each 1.0-mL cuvette contained 50 mM Hepes (pH 7.5), 0.1 M KCl, 2 mM D-glucose, 0.25 mM NADP, 5 mM excess $MgCl_2$, 25 units of hexokinase, 5 units of glucose-6-phosphate dehydrogenase, and various amounts of the different substrates and inhibitors. The reaction was initiated by the addition of 10–40 μg of glutamine synthetase.

Preincubation Studies and Substrate Activity of the Dead-End Inhibitors. To test whether or not the binding of the dead-end inhibitors to enzyme is reversible, millimolar concentrations of ACPS, APBA, and arsenate were preincubated with 20–40 μg of glutamine synthetase, buffer (pH 7.5), 0.1 M KCl, 5–6.25 mM $MgCl_2$, and, accordingly, 1 mM MgATP or 1–2 mM MgADP, 40 mM phosphate (with ACPS and APBA), and 50 mM glutamine (with arsenate). After incubation (30–60 min) at 25 °C, each mixture, along with an identical solution containing no inhibitor, was dialyzed overnight against 10–100 mM Hepes (pH 7.2), 0.1 M KCl, and 5 mM $MgCl_2$. The dialysates were then assayed for activity with the standard coupling enzyme mixtures. Under identical assay conditions, the activities of the mixtures which contained inhibitors were compared to the activities of the accompanying solutions which contained no inhibitors.

Each dead-end inhibitor was tested as an alternate substrate of glutamine synthetase. In both forward and reverse reactions, the substrate activity of ACPS and APBA was measured under normal assay conditions but in the absence of glutamate or glutamine. In all cases, alternate substrate activities were corrected for the residual enzyme activity that was observed in the absence of inhibitors.

The hexokinase–glucose-6-phosphate dehydrogenase assay could not be used to measure the substrate activity of arsenate since MgATP would not be a product of the reverse reaction in the absence of phosphate. Instead, substrate activity with arsenate was measured by the enzymatic determination of glutamate (Curthoys & Weiss, 1974). A 0.2-mL reaction mixture containing 50 mM Hepes (pH 7.5), 0.1 M KCl, 5 mM $MgCl_2$, 2 mM MgADP, 20 mM glutamine, 2 mM D-glucose, 5 units of hexokinase, (with and without) 12.5 mM potassium arsenate, and 56 μg of glutamine synthetase was incubated at 25 °C for 1 h. Hexokinase and glucose were present in order to shift the unfavorable equilibrium toward glutamate synthesis in the control mixture that contained phosphate. To this was added a 1.0-mL solution containing 50 mM Tris buffer (pH 8.6), 0.3 mM ADP, 4 mM NAD, 0.03% H_2O_2, 0.2 mM K^+-EDTA, and 82 units of glutamate dehydrogenase. After 30 min, the absorbance was read at 340 nm, and the glutamate concentration was determined from the amount of NADH formed.

Data Analysis. The kinetic data were analyzed by using the Fortran programs of Cleland (1967). Initial velocity data yielding an apparently intersecting pattern were fitted to eq 4 and parallel patterns to eq 5. For initial velocity experiments

$$v = \frac{VAB}{K_{ia}K_b + K_aB + K_bA + AB} \tag{4}$$

$$v = \frac{VAB}{K_aB + K_bA + AB} \tag{5}$$

where two changing fixed substrates were maintained in a fixed ratio, each line of the double-reciprocal plot was fitted to eq 6, and the resulting slopes and intercepts were replotted vs.

$$v = \frac{VA}{K + A} \tag{6}$$

the reciprocal concentration of either of the changing fixed substrates to determine whether the slope and intercept effects were linear or parabolic. In these cases, the nature of the slope and intercept effects was determined by comparison of the linear regressions of the slope and intercept replots vs. 1/(substrate) and 1/(substrate)^2. Competitive, noncompetitive, and uncompetitive inhibitions were fitted to eq 7, 8, and 9,

$$v = \frac{VA}{K(1 + (I/K_{is})) + A} \tag{7}$$

$$v = \frac{VA}{K(1 + (I/K_{is})) + A(1 + (I/K_{ii}))} \tag{8}$$

$$v = \frac{VA}{K + A(1 + (I/K_{ii}))} \tag{9}$$

respectively. When the type of pattern was in doubt for any

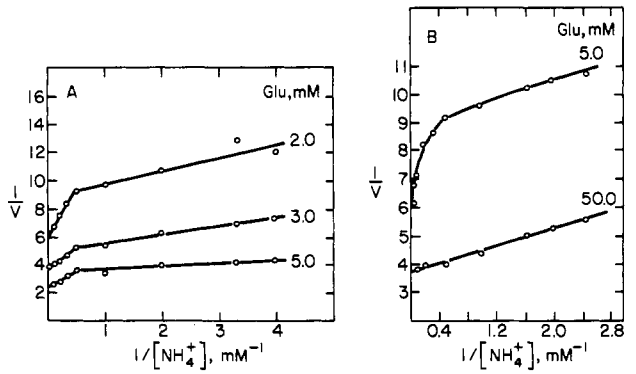

FIGURE 1: Initial velocity patterns with NH_4^+ as the varied substrate, glutamate as the changing fixed substrate, and with a saturating fixed MgATP concentration (10.0 mM). (A) NH_4^+ varied from 0.25 mM to 10.0 mM. The changing fixed glutamate concentrations were 2.0, 3.0, and 5.0 mM. (B) NH_4^+ varied from 0.4 mM to 50.0 mM with the ionic strength held constant above 10 mM NH_4^+ with KCl. Changing fixed glutamate concentrations are 5.0 and 50.0 mM. Other experimental conditions are the same as given for the standard assay. The velocities are in arbitrary units.

experiment, both possible fits were tried and a comparison of the σ values (square root of average residual least square) was made to determine the best fit. In no case did a set of data fit both patterns equally well. The nomenclature used in this paper is that of Cleland (1963).

Results

Nonlinear Initial Velocity Patterns with Varied Ammonium Ion. Shown in Figure 1A is the double-reciprocal plot of initial velocity with respect to ammonium ion at subsaturating changing fixed levels of glutamate and a saturating fixed level of MgATP (10 mM). A biphasic pattern is obtained which consists of two linear branches (0.25–1.0 mM NH_4^+ and 2.0–10.0 mM NH_4^+). When each of the linear portions is fitted with a K_m value, the K_m at the higher NH_4^+ concentrations (2.0–10.0 mM NH_4^+; $K_{NH_4^+}$ = 0.6 mM) is 10 times the value at the lower concentrations (0.25–1.0 mM NH_4^+; $K_{NH_4^+}$ = 0.06 mM).

Figure 1B shows that at fixed levels of 5 mM glutamate and 10 mM MgATP the curvature becomes more pronounced as NH_4^+ concentrations exceed 10 mM, and $K_{NH_4^+}$ should be even greater than 0.6 mM at these higher concentrations. Since the Michaelis constant increases progressively with increasing NH_4^+ concentrations, the usual effect of substrate saturation (zero-order kinetics when (A) $\gg K_a$) will not be observed. However, at 50 mM glutamate, the curved pattern becomes linear for the entire range of NH_4^+ concentrations ($K_{NH_4^+}$ = 0.2 mM). Variation of KCl concentrations (0–0.1 M) has no effect on the shapes of the two patterns in Figure 1, suggesting that the nonlinear kinetics observed with varied NH_4^+ is not due to an ionic-strength effect.

When NH_4^+ is varied (0.25–10.0 mM) at subsaturating changing fixed levels of MgATP, a biphasic plot (as in Figure 1A) is observed when the fixed glutamate level is subsaturating (5 mM), but the same pattern is completely linear throughout the range of NH_4^+ concentrations when the fixed glutamate level is saturating (100 mM). Thus, the appearance of biphasic double-reciprocal patterns with varied NH_4^+ depends on the fixed concentrations of glutamate and not on the fixed concentrations of MgATP.

When biphasic patterns (such as Figure 1A) were obtained, the pattern type (intersecting, parallel, noncompetitive, etc.) was determined by independently fitting each linear branch of the plot to the appropriate equation (see Materials and Methods), and, in all cases, the pattern type observed at low NH_4^+ concentrations (0.25–1.0 mM NH_4^+) was identical with that found at high NH_4^+ concentrations (2.0–10.0 mM). This treatment ensures that the kinetic behavior of NH_4^+ binding is consistent throughout the NH_4^+ concentration range examined in these experiments.

Initial Velocity Patterns. The initial velocity data for the forward and reverse reactions of glutamine synthetase are presented in Table I. The kinetic constants listed are from fits of the data to eq 4 and 5. For the forward reaction, NH_4^+ vs. MgATP gives an intersecting pattern that becomes parallel as the fixed glutamate level is raised from 3 mM (subsaturating) to 100 mM (saturating). Intersecting patterns are obtained with Glu vs. NH_4^+ at saturating MgATP, and MgATP vs. Glu at saturating NH_4^+. In the latter pattern, uncompetitive substrate inhibition is observed as the glutamate concentration reaches 50 mM, and the intercept inhibition constant (K_{ii}) for glutamate is 220 ± 70 mM (from a fit of the inhibited rates to eq 9).

In the reverse reaction, intersecting patterns are obtained with Gln vs. MgADP at subsaturating and saturating phosphate, phosphate vs. MgADP at 100 mM glutamine, and phosphate vs. Gln at saturating MgADP. When glutamine is varied at changing fixed concentrations of both MgADP and phosphate (fixed ratio MgADP/P_i = 1:20) and when phosphate is varied at changing fixed concentrations of both MgADP and glutamine (fixed ratio MgADP/glutamine = 1:40), intersecting patterns result in which the lines do not meet at a common point to the left of the $1/v$ axis. In the first of these patterns, a parabolic-slope effect and a linear-intercept effect are found when slopes and intercepts are replotted vs. 1/(phosphate) and 1/(phosphate)^2. From replots of the slopes and intercepts vs. 1/(Gln) and 1/(Gln)^2, the second pattern shows parabolism for both.

Product Inhibition Patterns. Product inhibition data from the forward reaction are shown in Table II. K_{is} and K_{ii} are the apparent slope and intercept inhibition constants, respectively, which are obtained from fits of the data to eq 7–9. Glutamine is a linear noncompetitive inhibitor of MgATP, glutamate, and NH_4^+. For the Gln vs. Glu pattern, raising the fixed level of either MgATP or NH_4^+ to saturation results in noncompetitive inhibition in which the slope effects are slightly larger than at subsaturating levels of these fixed substrates. The Gln vs. MgATP pattern also remains noncompetitive when the fixed glutamate level is raised to saturation. Phosphate inhibition is also linear noncompetitive vs. MgATP, glutamate, and NH_4^+. MgADP is a linear competitive inhibitor of MgATP and a linear noncompetitive inhibitor of glutamate and NH_4^+.

Preincubation Studies and Substrate Activity of Dead-End Inhibitors. In order to obtain reliable dead-end inhibition patterns with ACPS, APBA, and arsenate, it is necessary to demonstrate that none of these inhibitors is either an irreversible inactivator or an alternate substrate of glutamine synthetase. To show that the inhibitors combine with the enzyme reversibly, ACPS, APBA (forward and reverse assays), and arsenate (reverse assay) were incubated with glutamine synthetase and the other substrates at concentrations that greatly exceed both their respective inhibition constants and the molar concentration of enzyme catalytic sites. After inhibitors were removed by dialysis, the enzyme retained full activity. Hence, ACPS, APBA, and arsenate inhibit glutamine synthetase reversibly.

In reaction mixtures containing ATP, $MgCl_2$, NH_4Cl, and enzyme, the substrate activities of ACPS and APBA, as

Table I: Initial Velocity Patterns

A. Forward Reaction[a]

varied substrates	fixed substrate	pattern type	apparent Michaelis constants (mM) MgATP	Glu	NH_4^+
NH_4^+ vs. MgATP	Glu, 3 mM	intersecting	0.21 ± 0.05		0.01 ± 0.007
NH_4^+ vs. MgATP	Glu, 100 mM	parallel	2.0 ± 0.1		0.22 ± 0.01
MgATP vs. Glu	NH_4^+, 50 mM	intersecting	0.5 ± 0.2	3.7 ± 0.9	
Glu vs. NH_4^+	MgATP, 10 mM	intersecting		4.5 ± 0.5	0.06 ± 0.03

B. Reverse Reaction[b]

varied substrates	fixed substrate	pattern type	apparent Michaelis constants (mM) MgADP	Gln	phosphate
Gln vs. MgADP	phosphate, 2.4 mM	intersecting	0.064 ± 0.037	4.8 ± 0.9	
Gln vs. MgADP	phosphate, 100 mM	intersecting	0.044 ± 0.008	2.5 ± 0.2	
phosphate vs. MgADP	Gln, 100 mM	intersecting	0.053 ± 0.029		4.4 ± 1.5
phosphate vs. Gln	MgADP, 0.2 mM	intersecting		6.5 ± 1.2	3.0 ± 0.6
MgADP/phosphate vs. Gln		intersecting (S-parabolic, I-linear)			
MgADP/Gln vs. phosphate		intersecting (S-parabolic, I-parabolic)			

[a] At pH 7.5, 25 °C, 100 mM KCl, and 15–25 mM excess $MgCl_2$. Other conditions given in Materials and Methods. [b] At pH 7.5, 25 °C, 100 mM KCl, and 5–12 mM excess $MgCl_2$. Other conditions given in Materials and Methods.

Table II: Product Inhibition Patterns[a]

variable substrate	inhibitor	fixed substrate	inhibition pattern	K_{is} (mM)	K_{ii} (mM)
Glu	Gln	MgATP, 5 mM NH_4^+, 1 mM	NC	30 ± 3	65 ± 16
Glu	Gln	MgATP, 5 mM NH_4^+, 50 mM	NC	26 ± 2	170 ± 40
Glu	Gln	MgATP, 30 mM NH_4^+, 5 mM	NC	18 ± 3	170 ± 80
MgATP	Gln	Glu, 3 mM NH_4^+, 50 mM	NC	18 ± 1	29 ± 7
MgATP	Gln	Glu, 100 mM NH_4^+, 5 mM	NC	230 ± 70	340 ± 60
NH_4^+	Gln	MgATP, 5 mM Glu, 5 mM	NC	30 ± 7	43 ± 4
MgATP	phosphate	NH_4^+, 1 mM Glu, 3 mM	NC	45 ± 4	93 ± 9
Glu	phosphate	MgATP, 10 mM NH_4^+, 10 mM	NC	46 ± 3	176 ± 22
NH_4^+	phosphate	Glu, 5 mM MgATP, 5 mM	NC	84 ± 9	18 ± 4
MgATP	MgADP	Glu, 5 mM NH_4^+, 50 mM	C	1.12 ± 0.04	
Glu	MgADP	MgATP, 1 mM NH_4^+, 50 mM	NC	0.51 ± 0.06	5.0 ± 0.7
NH_4^+	MgADP	MgATP, 1 mM Glu, 3 mM	NC	0.7 ± 0.2	2.4 ± 0.2

[a] At pH 7.5, 25 °C, 100 mM KCl, and 15–25 mM excess $MgCl_2$. K_{is}, apparent slope inhibition constant; K_{ii}, apparent intercept inhibition constant; C, competitive inhibition; NC, noncompetitive inhibition; UC, uncompetitive inhibition. Other experimental conditions given in Materials and Methods.

compared to glutamate, are 0.06% and 1%, respectively. In assay mixtures containing ADP, $MgCl_2$, phosphate, and enzyme, the substrate activities of both ACPS and APBA are negligibly small compared to glutamine.

As an alternate substrate of phosphate in the reverse reaction, one would expect arsenate to displace the amide group of glutamine to form an unstable intermediate, γ-glutamyl arsenate. Decomposition of this intermediate by ADP attack in the same manner as with γ-glutamyl phosphate would lead to the formation of glutamate but not ATP. For this reason, any substrate activity with arsenate will not be detected by the hexokinase–glucose-6-phosphate dehydrogenase assay but can be determined from the amount of glutamate produced in the reaction. In a reaction mixture containing ADP, glutamine, $MgCl_2$, and enzyme, the amount of glutamate formed from arsenate is 1% of that formed from a comparable concentration of phosphate. This is under the normal conditions of the reverse biosynthetic reaction assay, using hexokinase and glucose to pull the reaction to completion. In the absence of hexokinase, arsenate activity is 60% of the (greatly decreased) phosphate activity.

None of the three inhibitors possesses substrate activity greater than 1%. These activities are too low to result in a significant alternate substrate pathway, so as a result, the dead-end inhibition patterns obtained with ACPS, APBA, and arsenate are straightforward.

Dead-End Inhibition Patterns. The inhibition patterns with ACPS, APBA, and arsenate for both forward and reverse reactions are shown in Table III. All patterns give linear inhibition. The apparent slope and intercept inhibition constants are from fits of the data to eq 7–9. In studies of the forward reaction, both ACPS and APBA are competitive vs. glutamate, noncompetitive vs. NH_4^+, and uncompetitive vs. MgATP. The inhibition constants of ACPS and APBA are

Table III: Dead-End Inhibition Patterns

variable substrate	inhibitor	fixed substrate	inhibition pattern	K_{is} (μM)	K_{ii} (μM)
		A. Forward Reaction[a]			
MgATP	ACPS	Glu, 3 mM NH_4^+, 50 mM	UC		82 ± 5
Glu	ACPS	MgATP, 5 mM NH_4^+, 50 mM	C	51 ± 4	
NH_4^+	ACPS	MgATP, 5 mM Glu, 3 mM	NC	29 ± 4	115 ± 8
MgATP	APBA	Glu, 3 mM NH_4^+, 50 mM	UC		71 ± 3
Glu	APBA	MgATP, 5 mM NH_4^+, 50 mM	C	54 ± 2	
NH_4^+	APBA	MgATP, 5 mM Glu, 3 mM	NC	26 ± 5	58 ± 4
		B. Reverse Reaction[b]			
Gln	ACPS	MgADP, 2 mM phosphate, 50 mM	C	177 ± 14	
Phosphate	ACPS	MgADP, 2 mM Gln, 2.5 mM	NC	82 ± 16	266 ± 76
MgADP	ACPS	Gln, 2.5 mM phosphate, 50 mM	UC		225 ± 19
Phosphate	arsenate	MgADP, 2 mM Gln, 50 mM	C	82 ± 6	
Gln	arsenate	phosphate, 2 mM MgADP, 2 mM	UC		75 ± 5
MgADP	arsenate	Gln, 50 mM phosphate, 2 mM	UC		38 ± 2

[a] At pH 7.5, 25 °C, 100 mM KCl, 20–25 mM excess $MgCl_2$. Other conditions given in Materials and Methods. [b] At pH 7.5, 25 °C, 100 mM KCl, 3–5 mM excess $MgCl_2$. Other conditions given in Materials and Methods.

51 ± 4 μM and 54 ± 2 μM, respectively, indicating that their binding to glutamine synthetase is substantially tighter than glutamate's (K_m = 4 mM). For the reverse reaction, ACPS is a competitive inhibitor of glutamine with an inhibition constant of 177 ± 14 μM. ACPS is noncompetitive vs. phosphate and uncompetitive vs. MgADP. Arsenate is a competitive inhibitor of phosphate with an inhibition constant of 82 ± 6 μM. Inhibition vs. both MgADP and glutamine is uncompetitive.

Discussion

Nonlinear Double-Reciprocal Plots with Variable NH_4^+. The occurrence of nonlinear double-reciprocal plots that are concave downward at high concentrations of the varied substrate is not uncommon for multisite enzymes. This behavior is often referred to as substrate activation, and kinetic patterns of this general form indicate that the varied substrate can combine with more than one form of the enzyme. This situation may arise in several instances: (1) when two distinct enzymes are present that catalyze the same reaction, (2) when substrate combination with the enzyme is steady-state random, (3) when separate regulatory sites exist for the varied substrate, or (4) when cooperative effects between subunits change the enzyme's affinity for the varied substrate (Cleland, 1970).

Of these possibilities, the most likely is negative cooperativity of NH_4^+ binding. Boyer has recently reported a cooperative interaction between NH_4^+ and the *E. coli* enzyme (Boyer, 1980). The appearance of biphasic curves in kinetic plots has been attributed to negatively cooperative substrate binding in rabbit muscle glyceraldehyde-3-phosphate dehydrogenase (Conway & Koshland, 1968), beef liver glutamate dehydrogenase (Olson & Anfinsen, 1953), deoxythymidine kinase (Okazaki & Kornberg, 1964), and bovine liver argininosuccinate synthetase (Rochovansky et al., 1977). In the last two of these examples, the degree of negatively cooperative binding of one substrate is dependent upon the fixed concentration of another substrate in the same manner as the glutamate–ammonia interdependence of glutamine synthetase.

Scheme I

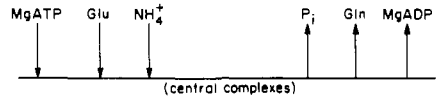

Since negative cooperativity allows the enzyme to be insensitive to large fluctuations in physiological ammonia concentrations, the enzyme maintains an efficient response to a wide range of ammonia concentrations when glutamate levels are low. However, when glutamate is saturating, the cooperativity vanishes and the enzyme is more sensitive to extremes of ammonia concentration. By deactivating the enzyme's cooperative ammonia binding, glutamate, to some extent, regulates enzyme activity with respect to the availability of substrates. This type of substrate interedependence can be seen as exerting a versatile control over *E. coli* glutamine synthetase, adding further complexity to the already intricate regulation of this enzyme.

Kinetic Mechanism. The kinetic mechanism that is most consistent with the above data is the ordered ter-ter mechanism shown in Scheme I. A full rate equation for this mechanism can be found in Segel (1975).

This mechanism is derived from the following observations:

(1) The initial velocity patterns for MgATP vs. Glu and Glu vs. NH_4^+ are both intersecting, and the NH_4^+ vs. MgATP is intersecting at low glutamate but parallel at saturating glutamate. These patterns conform to an ordered combination of the substrates in which glutamate is the second substrate to bind. The uncompetitive substrate inhibition observed at high glutamate concentrations in the MgATP vs. Glu pattern is characteristic of an ordered mechanism and probably arises from the dead-end combination of glutamate with an enzyme–product transitory complex such as E-MgADP.

(2) ACPS and APBA are both competitive inhibitors vs. glutamate, uncompetitive inhibitors vs. MgATP, and noncompetitive inhibitors vs. NH_4^+. These patterns indicate an ordered addition of substrates: MgATP, glutamate, and NH_4^+.

Scheme II

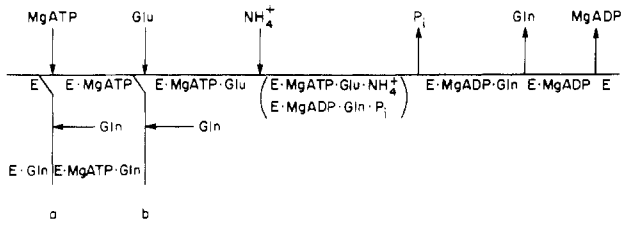

(3) Phosphate is a noncompetitive inhibitor vs. MgATP, glutamate, and NH_4^+, indicating that it is the first product released from central complexes.

(4) MgADP is a competitive inhibitor vs. MgATP and a noncompetitive inhibitor vs. glutamate and NH_4^+. Therefore MgATP and MgADP both bind to free enzyme.

(5) Although all initial velocity patterns in the reverse reaction are intersecting, the low solubility of glutamine may have prevented holding it at a fixed concentration high enough to convert the intersecting phosphate vs. MgADP pattern to a parallel one. When the method of Rudolph & Fromm (1969) is used, the initial velocity pattern of MgADP and phosphate (held in a fixed ratio of 1:20) vs. glutamate is intersecting with a parabolic-slope effect and a linear-intercept effect. This result suggests that the substrates of the reverse reaction also combine with enzyme in an ordered manner and glutamine is the second substrate to bind.

(6) ACPS is a competitive inhibitor vs. glutamine, an uncompetitive inhibitor vs. MgADP, and a noncompetitive inhibitor vs. phosphate. The order of substrate addition in the reverse reaction is MgADP, glutamine, and phosphate.

(7) Arsenate is a competitive inhibitor vs. phosphate and an uncompetitive inhibitor vs. both MgADP and glutamine. This confirms the binding order of substrates given in (6). Arsenate has been shown to be an alternate substrate of the reverse reaction of *E. coli* glutamine synthetase, with an activity of nearly 50% relative to phosphate (Rhee et al., 1976). We found arsenate activity to be only 1% of phosphate substrate activity, but the reason for this is that under our experimental conditions hexokinase and glucose immediately remove the product ATP and shift the unfavorable equilibrium toward glutamate synthesis. The alternate substrate pathway of arsenate is then insignificant compared to phosphate activity, and so the inhibition patterns observed are solely the result of dead-end complex formation.

The mechanism of Scheme I predicts that all product inhibition patterns with glutamine will be uncompetitive, but every observed glutamine inhibition is noncompetitive. The appearance of noncompetitive patterns suggests that glutamine either is released from central complexes randomly with phosphate, forms dead-end complexes with enzyme–substrate transitory complexes, or binds to an inhibitory allosteric site. If glutamine is released from central complexes, an uncompetitive inhibition pattern should be observed for Gln vs. Glu at saturating NH_4^+ (50 mM) and for Gln vs. MgATP at saturating glutamate (100 mM). However, noncompetitive inhibition persists in both of these patterns, a result which is inconsistent with either totally ordered or partially random product release.

At the high glutamine concentrations needed to observe product inhibition, it is likely that glutamine also binds to either an incorrect enzyme form in a dead-end fashion or an inhibitory allosteric site. For dead-end complex formation, E-MgATP-Gln (Scheme II, path b) would seem to be the most probable complex, but the noncompetitive Gln vs. MgATP pattern at 100 mM glutamate (a glutamate concentration sufficient to convert the intersecting NH_4^+ vs. MgATP pattern into a parallel one) eliminates it as a possibility. Noncompetitive inhibitions vs. all substrates would be observed if glutamine forms a dead-end complex with free enzyme (Scheme II, path a). Saturation with MgATP should preclude E-Gln formation, but, in the noncompetitive Gln vs. Glu patterns, the slope effect actually increases as the fixed MgATP concentration is raised from 5 to 30 mM. However, since MgATP and glutamine occupy different subsites on the enzyme, saturating MgATP may not totally prevent the combination of free enzyme and glutamine. Alternatively, the noncompetitive inhibition patterns may be caused by the interaction of glutamine with an allosteric site such that the Michaelis constants of the substrates are raised.

The proposed kinetic mechanism is consistent with a reaction pathway involving partial reactions 2 and 3, although it is impossible to determine from steady-state methods whether γ-glutamyl phosphate is formed before or after ammonia binds. Since the product MgADP apparently does not dissociate from the putative E·MgADP·γ-Glu-P complex, the kinetic mechanism is a sequential one, and the ordered mechanism of Scheme I predicts that MgATP $\rightleftarrows$ MgADP isotope exchange should not be observed in the absence of ammonia because the nucleotides cannot leave the enzyme before the amino acids. Thus, the tight binding of γ-glutamyl phosphate prevents MgADP dissociation prior to its reaction with ammonia. The formation of tightly bound γ-glutamyl phosphate is also indicated by positional isotope exchange studies (Midelfort & Rose, 1976). Here, scrambling of the isotope in the β,γ bridge of [^{18}O]ATP requires only the presence of glutamate and does not lead to ADP formation. This demonstrates that chemistry occurs between ATP and glutamate in the absence of ammonia without resulting in ADP release, a result which agrees with the findings of Weisbrod & Meister (1973).

The binding constants of the dead-end inhibitors ACPS and APBA (K_i = 50 μM) are two orders of magnitude lower than that of glutamate (K_m = 4 mM), and these binding constants would presumably be smaller still for the resolved L-amino acid analogues. Since the tetrahedral geometry of the sulfur and phosphorus atoms of ACPS and APBA, respectively, should structurally mimic a tetrahedral adduct of γ-glutamyl phosphate and ammonia (III), the tight binding of these glutamate analogues strongly suggests that the enzyme stabilizes the formation and binding of such an adduct. Further support for a sequential mechanism involving two covalent intermediates (such as γ-glutamyl phosphate and III) comes from fast kinetic studies in which the binding of all three substrates to enzyme is followed by the formation of two fluorometrically distinct intermediates, the second of which is consumed linearly with increasing ammonia concentration (Rhee & Chock, 1976).

The ordered ter-ter mechanism is in disagreement with the steady-state random mechanism suggested by equilibrium isotope exchange experiments (Wedler & Boyer, 1972). The substantial difference in experimental pH between the isotope exchange experiments (pH 6.5) and our initial rate data (pH 7.5) probably does not account for the discrepancy in kinetic mechanism since recent isotope exchange data also indicate random binding at pH 7.5 (F. C. Wedler, 1979, private communication). Isotope exchange is an inherently more sensitive technique for detecting alternate pathways in ostensibly ordered mechanisms than are normal initial rate methods. Whereas all initial rate data may indicate a totally ordered mechanism, the observation of either partial or no substrate inhibition in isotope exchange patterns (as with glutamine

synthetase) suggests that alternate pathways are available. Careful studies of alcohol dehydrogenase (Ainslie & Cleland, 1972) and hexokinase (Danenberg & Cleland, 1975) have shown both enzymes to be steady-state random with preferred ordered pathways, and these findings reconcile the disparity between the results of initial rate and isotope exchange studies of these enzymes.

In view of such examples, the kinetic mechanism of *E. coli* glutamine synthetase appears to be steady-state random with a preferred ordered ter-ter pathway. It is possible that catalysis occurs exclusively through this ordered pathway, and the absence of substrate-inhibited isotope exchange patterns is due entirely to spurious dissociations of the nucleotides and amino acids from the transitory and central complexes. In other words, MgATP and glutamate may not be completely trapped on the enzyme by ammonia binding as is required for a compulsory ordered mechanism. Also glutamate binding may not totally prevent MgATP dissociation from the ternary E–MgATP–Glu complex. The fact that saturating NH_4^+ cannot completely suppress positional isotope exchange in [^{18}O]ATP, as would be expected for compulsory ordered binding, may be due in part to dissociation of ATP (that has undergone positional isotope exchange) from the quaternary E–MgATP–Glu–NH_3 complex. It should be possible to quantitate the extent to which this is occurring by the isotope partitioning method (Rose et al., 1974). The amount of radioactive MgATP and radioactive glutamate that are trapped by glutamate and ammonia, respectively, should reveal how much those labeled substrates can dissociate "out of turn" from the central and ternary complexes.

The ordered mechanism of *E. coli* glutamine synthetase we have presented here adds a new dimension to the existing kinetic data of this enzyme, tending to classify it, along with hexokinase and alcohol dehydrogenase, as a random enzyme with a preferred ordered pathway. More studies on other enzymes may demonstrate that preferred ordered pathways are the rule for random enzymes whose rate-determining step is not interconversion of the central complexes.

Acknowledgments

We are deeply indebted to Dr. Frank Raushel for his assistance with data analysis and to Laurel B. Bernstein for excellent technical assistance.

Supplementary Material Available

Six double-reciprocal plots: NH_4^+ vs. MgATP at 3 mM glutamate; NH_4^+ vs. MgATP at 100 mM glutamate; MgATP vs. Glu at 50 mM NH_4^+ showing substrate inhibition by glutamate; arsenate vs. P_i; arsenate vs. MgADP; ACPS vs. Gln (3 pages). Ordering information is given on any current masthead page.

References

Ainslie, G. R., & Cleland, W. W. (1972) *J. Biol. Chem. 247*, 946.

Allison, R. D., Todhunter, J. A., & Purich, D. L. (1977) *J. Biol. Chem. 252*, 6046.

Boyer, P. D. (1980) *Fed. Proc., Fed. Am. Soc. Exp. Biol. 39*, 1822.

Cleland, W. W. (1963) *Biochim. Biophys. Acta 67*, 104.

Cleland, W. W. (1967) *Adv. Enzymol. Relat. Areas Mol. Biol. 29*, 1.

Cleland, W. W. (1970) *Enzymes, 3rd Ed. 2*, 1.

Conway, A., & Koshland, D. E. (1968) *Biochemistry 7*, 4011.

Curthoys, N. P., & Weiss, R. F. (1974) *J. Biol. Chem. 249*, 3261.

Danenberg, K. D., & Cleland, W. W. (1975) *Biochemistry 14*, 28.

Fromm, H. J. (1967) *Biochim. Biophys. Acta 139*, 221.

Ginsburg, A., Yeh, J., Hennig, S. B., & Denton, M. D. (1970) *Biochemistry 9*, 633.

Krishnaswamy, P. R., Pamiljans, V., & Meister, A. (1962) *J. Biol. Chem. 237*, 2932.

Lowry, O. H., Rosebraugh, N. J., Farr, A. L., & Randall, R. J. (1951) *J. Biol. Chem. 193*, 235.

Meek, T. D. (1980) *Fed. Proc., Fed. Am. Soc. Exp. Biol. 39*, 2032.

Meek, T. D., & Villafranca, J. J. (1978) *12th Middle Atlantic Regional Meeting of the American Chemical Society, Abstr. P55.*

Midelfort, C. F., & Rose, I. A. (1976) *J. Biol. Chem. 251*, 5881.

Miller, R. E., Shelton, E., & Stadtman, E. R. (1974) *Arch. Biochem. Biophys. 163*, 155.

Mosher, C. W., Silverstein, R. M., Crews, O. P., & Baker, B. R. (1958) *J. Org. Chem. 23*, 1257.

Okazaki, R., & Kornberg, A. (1964) *J. Biol. Chem. 239*, 275.

Olson, J. A., & Anfinsen, C. B. (1953) *J. Biol. Chem. 202*, 841.

Reisner, D. B. (1956) *J. Am. Chem. Soc. 78*, 5702.

Rhee, S. G., & Chock, P. B. (1976) *Proc. Natl. Acad. Sci. U.S.A. 73*, 476.

Rhee, S. G., Chock, P. B., & Stadtman, E. R. (1976) *Biochimie 58*, 35.

Rochovansky, O., Kodowaki, H., & Ratner, S. (1977) *J. Biol. Chem. 252*, 5287.

Rose, I. A., O'Connell, E. L., Litwin, W., & BarTana, J. (1974) *J. Biol. Chem. 249*, 5163.

Rudolph, B. F., & Fromm, H. J. (1969) *J. Biol. Chem. 244*, 3832.

Segel, I. H. (1975) *Enzyme Kinetics*, p 700, Wiley-Interscience, New York.

Shapiro, B. M., & Stadtman, E. R. (1970) *Methods Enzymol. 17A*, 910.

Stadtman, E. R., & Ginsburg, A. (1974) *Enzymes, 3rd Ed. 10*, 755.

Timmons, R. B., Rhee, S. G., Luterman, D. L., & Chock, P. B. (1974) *Biochemistry 13*, 4479.

Tsuda, Y., Stephani, R. A., & Meister, A. (1971) *Biochemistry 10*, 3186.

Wedler, F. C., & Boyer, P. D. (1972) *J. Biol. Chem. 247*, 984.

Weisbrod, R., & Meister, A. (1973) *J. Biol. Chem. 248*, 3997.

Woolfolk, C. A., Shapiro, B. M., & Stadtman, E. R. (1966) *Arch. Biochem. Biophys. 116*, 177.